LABORATORY WORK ON THE SHAPE OF ASTEROIDS

J. L. Dunlap

Submitted to the Faculty of the

DEPARTMENT OF ASTRONOMY

In Partial Fulfillment of the
Requirements For the Degree of

MASTER OF SCIENCE

In the Graduate College

UNIVERSITY OF ARIZONA

1972

Accepted as a Master's Thesis,

Elizabeth Roemer

Myron Gehrels

Walter S. Fitch

June 28, 1972

ABSTRACT

Fourteen models were constructed and observed in the laboratory for light variation at different orientations of the rotation axis relative to the detector and the light source. In all, 311 lightcurves were obtained for elongated models with fairly uniform surface reflectivities. While there are some lightcurve features that may be used to distinguish between differences in the shape of the models, it is necessary first to know the position of the rotation axis with good precision (up to $\pm 1^{\circ}$ for highly elongated bodies). In general, there is no amplitude-aspect function characteristic of each model, but approximate relations may be used if the phase angles are $< 20^{\circ}$ and if the maximum lightcurve amplitude is $\geq 0^{m}.4$. The model data are compared to the observations of Hektor and Geographos and suggest that Hektor may be a double body, and that Geographos is about three times longer than it is wide. Shifts in the arrival times of the lightcurve maxima of one of the models were used to obtain the orientation of the rotation axis and sidereal period of Geographos. An equation for this time shift, which agrees with most of the model observations, is given and should be used in correcting epochs of maximum light in lightcurves of elongated asteroids.

I. INTRODUCTION

Photometric lightcurves of about 60 asteroids have been obtained over the past twenty years, yet very little is known about the shape of these objects. Some of the difficulties are described in a review of the work on Eros by Vesely (1971). References for photometric lightcurves are summarized in Table I of Taylor (1971). These lightcurves exhibit a wide variety of shapes - even for lightcurves of the same object observed at different oppositions. The general problem is to distinguish between the effects of shape and reflectivity differences on the light variation and to construct a three-dimensional picture of the asteroid. Russell (1906) concluded, for the general problem, that "it is impossible to determine the shape of an asteroid" from the light variation alone. His analysis, however, did not include the case of constant reflectivity and variable shape. Now that precise photometric lightcurves of 60 asteroids are available, it is possible to consider what is probable regarding the interpretation of the lightcurves, and thereby establish certain criteria which restrict the general problem to those cases for which some information about the shape may be determined from the lightcurves alone. Moreover, simultaneous measurements of polarization and light variation may permit the discrimination of shape versus reflectivity effects.

Most asteroids have rotation periods averaging about eight hours and have two maxima and two minima in a complete lightcurve. The maxima are generally at about the same level, and the minima may differ by a somewhat greater amount. Van Houten (1965) has noted that when the amplitude exceeds $0^m.2$, the average difference between the maxima (or minima) is about $0^m.04$, which represents the relative

importance of reflectivity differences between the two opposite sides (or ends). Lightcurves with large amplitudes ($>0^m.4$) always have wide rounded maxima and usually narrow sharp minima, while lightcurves with small amplitudes ($<0^m.2$) usually have rounded maxima and minima. Thirty-three asteroids have been observed at more than one longitude, and 23 of these have lightcurves whose amplitude changes with longitude.

On the basis of the above observations, the following assumptions seem reasonable.

a) Most asteroids are not spherical. The appearance of two maxima and two minima is more likely due to a change in cross-sectional area than to a pattern of bright and dark regions, which would most likely produce only one maximum and one minimum, or possibly several smaller maxima and minima.

b) Asteroids with lightcurves having large amplitudes and sharp minima are most likely elongated objects. A very unlikely pattern of bright and dark regions would be required to produce the sharp minima and two maxima and two minima in one period. The lightcurve of Iapetus (large amplitude and sharp minimum) is apparently due to one side being bright and the other dark (Widorn, 1952; Zellner, 1972). However, there is only one maximum and one minimum in one period.

Table I is a preliminary classification of asteroids into three categories, depending on the probable degree of the relative dominance of shape versus reflectivity effects in the lightcurves. The first class, of which (624) Hektor is a typical example, is shape dominated. The second class is probably shape dominated, but there may be reflectivity effects also present. An example of this class

TABLE I. A CLASSIFICATION OF ASTEROID LIGHTCURVES

I.	II.		III.	
15	6	43	1	25 ?
39 ?	7	45	2	29
44	9	61	3	51
321 ?	12	89	4	60
433	17	162	5	532 ?
624	18	349	8	1566
1620	19	354	10	
1971 FA	20	511	11	
	22	911	14	
	42	1437	23 ?	

The three classes are defined as follows:

I. Shape dominated. Objects are elongated.

II. Probably shape dominated.

III. Probably reflectivity dominated. Objects are nearly spherical.

is (22) Kaliope, although it is difficult to describe an average member of this group. The third class is nearly spherical and relatively large reflectivity effects are likely. An example of an asteroid with a smooth lightcurve is (4) Vesta; (29) Amphitrite has an unusually ragged lightcurve. Objects not included in the list have been oberved at only one opposition and the lightcurves are inconclusive regarding possible classification. (See Taylor, 1971.)

The purpose of this classification is to identify those particular asteroids whose light variation is caused mostly by the shape (class I). The object of this investigation is to identify the effects of shape on lightcurves using laboratory models with nearly uniform reflectivity, and to try to build a model that can reproduce the observed lightcurves of a particular asteroid ((1620) Geographos). The results should apply to the other members of class I, to a lesser extent class II, and may have little relevance to class III. Some of this work was published in a preliminary report (Dunlap, 1971).

II. EXPERIMENTAL DESIGN

The equipment used to produce lightcurves of model asteroids in the laboratory was a model support, light source, detector, and a data recording system. Fig. 1 shows the model support, designed by the author and built by Mike Arthur of the Lunar and Planetary Laboratory in the summer of 1970. A stepping motor turned the axis of rotation of the model by as little as 0.4° per step, and the angle of rotation was read out on a digital volt meter (dvm) through a continuously rotating potentiometer calibrated from 0° - 360°. The gap at the end of the resistance wire caused a small uncertainty in determining the angle of rotation as the sliding contact crossed

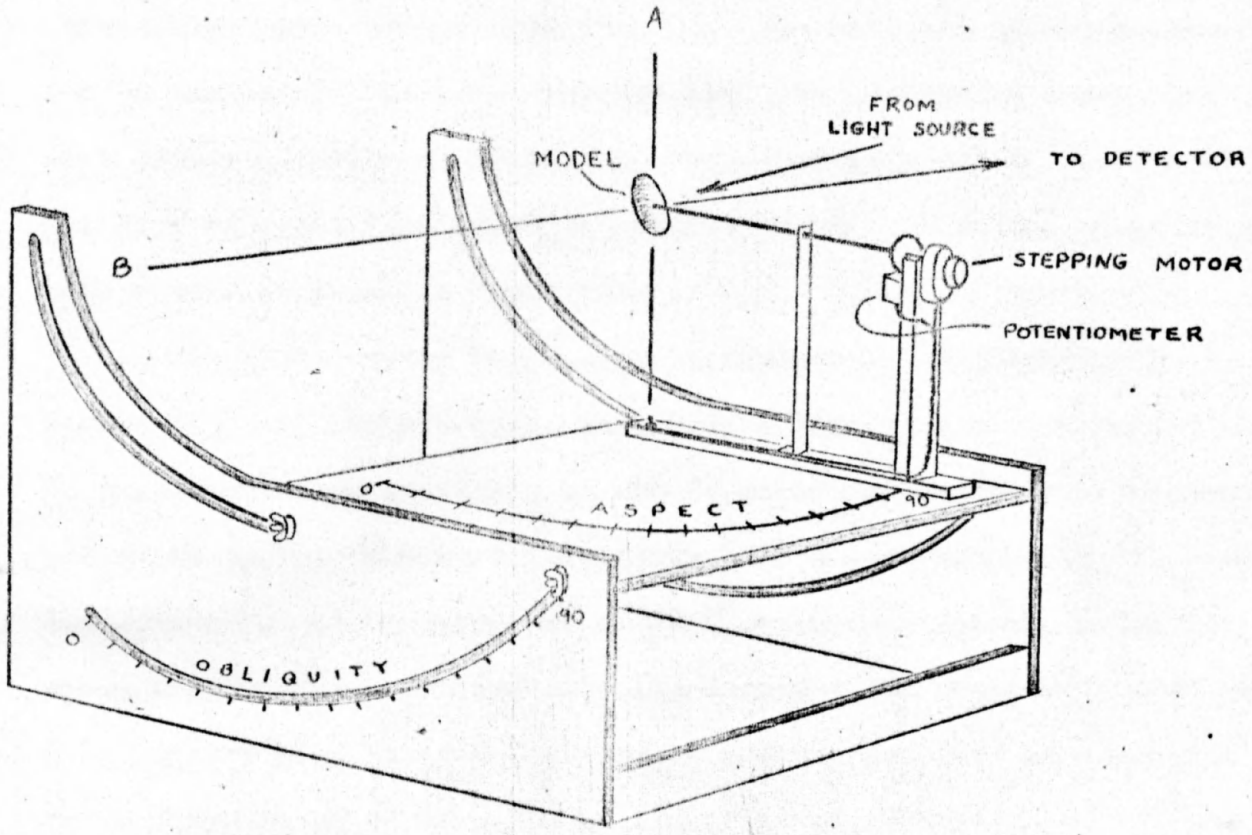

Fig. 1. The model support.

the gap. Consequently the angle on the dvm was at most 2% larger than the true angle of rotation by the end of one period. Apart from this systematic error, the angles were measured to the nearest degree ($\pm 0.3^{\circ}$ est. p.e.).

The model axis can be oriented in space about two other axes through the model center (see Fig. 1). One axis (A) is perpendicular to the top of the model support box, and a rotation about this axis causes a change in "aspect". The other axis (B) is horizontal - the line of sight from model to detector - and a rotation about this axis causes a change in "obliquity".

The light source was a 12 volt automobile headlight bulb housed in a baffled stovepipe tube 3.05 m long with a diameter of 18 cm. Mounted on a tripod, it can be moved horizontally to change the phase angle. The bulb itself was 3.67 m from the model, so that the divergence of the beam was about 1° across an average model dimension (~6 cm). Although the light source did not give a beam of uniform intensity in cross-section at a plane centered on the model and perpendicular to the line of sight to the detector, the difference in the integrated intensity between horizontal and vertical cross-sections having an area intermediate between the maximum area of models 2 and 3 was about 1% for a 20° phase angle. The ends of the most elongated models were closer to the light and detector than the sides for certain model orientations (large aspects); this caused the minima to be at most 2% brighter than they would, had the light source been infinitely far away. The light source was periodically checked for intensity variation by reobserving the model in the same orientation. The estimated error associated with any such variation was less than $0^{m}.01$. The light source and tube

were rotated 90° about the long axis of the tube to see if there would be an difference in the equatorial lightcurves as the model turned through different sections of the light beam. No difference was observed in the lightcurves.

The models were imaged on the photo-cathode with a lens mounted in front of the detector which was located about 3.7 m from the model. The detector and the digital recording system were the same gear that is used for polarimetric observation at the telescope (Coyne and Gehrels, 1967). No filter was used, and the polarimeter was locked in one position. The observations were made in a dark room and the photomultiplier tubes were operated at room temperature. The dark current was measured at the end of each lightcurve, and the change was negligible. A black cloth was hung on the wall behind the model (out of the light beam) and background readings were made once for each different phase angle for the first model by removing the model from the axis. The readings were small and nearly constant, so they were made less frequently for the other models to save time and to decrease the chances of damaging the models. The mean background reading was subtracted in the reductions of the lightcurves.

In all, 14 models were built and observed. Fig. 2 shows some of the first models tested. (The one at the left was not used.) They were built with styrofoam centers, covered with a thin layer of Plasticene, and then dusted with powdered rock and allowed to cure until the oil of the Plasticene had saturated the powder, making the model as tested noticably darker than when freshly powdered. This resulted in a fairly uniform reflecting surface reasonably free of obvious dark or light spots. Table II contains a description of the

Fig. 2. Some early models.

TABLE II. DESCRIPTION OF THE MODELS

No.	Shape	Dimensions		$\frac{A_{max}}{A_{min}}$	Remarks	Fig. 2 (from right)
1	Two "tangent" spheres of equal diameters	Sphere diameters Width of contact region	4.5 cm 1.8 cm	2.01	The contact region around the point of tangency was filled in for added strength.	1
2	Cylinder with hemispherical ends	Length Width	8.2 cm 4.5 cm	1.92		5
3	Cylinder with hemispherical ends	Length Width	11.9 cm 2.8 cm	4.56		3
4	Cylinder with conical ends	Length Width	(~9 cm) 4.5 cm		This model was converted into model 8 before it was measured.	
5	Cylinder with hemispherical ends, surface rough with lumps and pits	Length Width Variations	11.9 cm 3.2 cm ± 0.4 cm	3.93	Overall roughness was made by rolling it on a brick; then some larger bumps were added.	4
6	Rectangular solid	Length Width Height	11.2 cm 2.8 cm 2.7 cm	3.88		6
7	Model 3 with one end and part of one side darkened with graphite powder.					

TABLE II. Continued

No.	Shape	Dimensions		$\frac{A_{max}}{A_{min}}$	Remarks	Fig. 2 (from right)
8	Cylinder with one end conical & other end hemispherical	Length Width Cone height	8.7 cm 4.5 cm 4.4 cm	1.80		2
9	Two tangent spheres of unequal diameters	Diameter a Diameter b Width of contact region	6.1 cm 2.8 cm 2.1 cm	1.20	The rotation axis was located near the center of mass; the small sphere was near the equator of the rotation.	
10	Elongated, irregular	Length Width Variations	6.5 cm 4.0 cm $\pm$ 0.6 cm	1.50	Surface covered with craters of 1 - 2 cm diameter separated by fairly steep ridges.	
11	Three-axis "ellipsoid"	Length Width Height	6.5 cm 4.6 cm 3.5 cm	1.98	Rotation axis was along the shortest body dimension.	
12	Peculiar "elbow" shape with rounded corners & rounded edges	Length Width a Width b Width c Height	8.9 cm 6.0 cm 3.2 cm 3.9 cm 3.2 cm	1.68	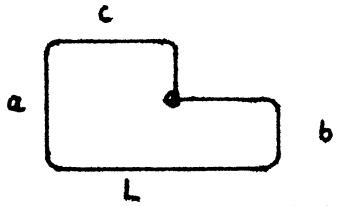	

TABLE II. Continued

No.	Shape	Dimensions		$\frac{A_{max}}{A_{min}}$	Remarks
13	Cylinder with hemispherical ends	Length Width	3.3 cm 1.2 cm	3.21	
14	Two tangent "ellipsoids"	Length (2a) a/b Width of contact region	3.9 cm 1.63 cm 1.4 cm	3.26	Point of tangency at ends of the long axes

models including their shapes, dimensions, ratio of maximum to minimum projected area and in the last column their position from the right in Fig. 2 (for those pictured there).

III. MODEL LIGHTCURVE DATA

The lightcurve observations required two observers - one to orient the model and operate the stepping motor, and the other to check the centering and code each angle for the digital punch. About three lightcurves were made each hour. Six of the models were observed at 3° intervals over 240° of rotation and six at 5° intervals over 360°. The first four angles were repeated at the end of each lightcurve as a check. For each of the first eight models (Table II), 27 lightcurves were made for the various combinations of "aspect" (90°, 60°, 35°), "astrocentric obliquity" (15°, 50°, 90°) and "phase" (20°, 40°, 60°). Fig. 3 defines each of these parameters in the laboratory coordinate system. With models 9 - 12, the nine lightcurves at 60° phase were omitted. The latter two models were each observed at four pre-determined orientations (Sec. V). Additional lightcurves of model 7 were obtained for additional obliquities for which the light source was placed on the other side of the line of sight from model to detector. The lightcurves were reduced and plotted in magnitude units on the IBM 1130 of the Lunar and Planetary Laboratory.

Table III is a summary of the lightcurve data of the 12 models observed systematically in aspect, astrocentric obliquity, and phase. The first column gives the identification according to the following code:

First digit: aspect

$1 = 90^\circ$; $2 = 60^\circ$; $3 = 35^\circ$

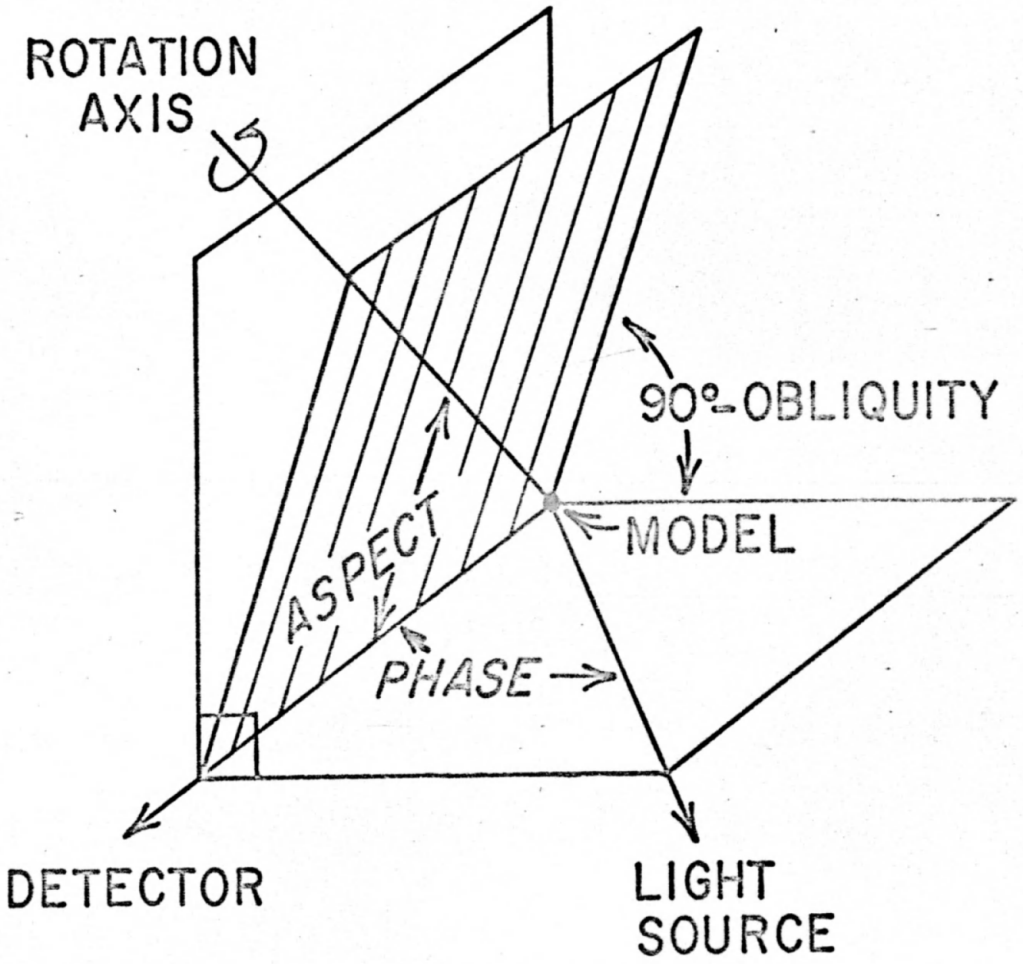

Fig. 3. The geometry of the laboratory observations.

Second digit: astrocentric obliquity

1 = 90°; 2 = 50°; 3 = 15°; 4 = -165°; 5 = -130°; 6 = -90°

Third digit: phase

1 = 20°; 2 = 40°; 3 = 60°

The next three or four columns give the angle of rotation of the model at which the epochs listed occurred. The time shift identifies the shift in degrees of maximum I relative to that epoch for the first lightcurve (ID 111). Positive shifts indicate a later arrival. The column labeled amp I gives the amplitude (in magnitude units) from the highest maximum to the lowest minimum. For some models, amp II was also observed, and this is the amplitude from the highest maximum to the highest minimum. The next to last column (1/2 width min) gives the width of the minimum in degrees at half amplitude. For models 1 - 8, the precision of the angle measurements in Table III is $\pm 1^{\circ}$ (est. p.e.); for models 9 - 12 it $\pm 2^{\circ}$ (est. p.e.). The precision of the amplitudes is $\pm\ 0^{m}.01$ (est. p.e.). Colons are used whenever the error is at least three times larger. Identification of the epochs becomes more uncertain as the amplitude approaches zero.

TABLE III. LIGHTCURVE DATA Model 1

ID	Max I	Min	Max II	Time Shift	Amp. I	1/2 Width Min	Remarks
111	72°	164°	256°	0°	0m.80	50°	
211	77	166	266	5	.20	76	
311	116	196	283	44	.06	84	
121	81	164	265	9	.82	51	
221	86	165	267	14	.26	80	
321	84	172	266	12	.12	96	
131	83	164	264	11	.82	59	
231	81	166	264	9	.30	80	
331	66	150	248	-6	.10	100	
112	72	164	258	0	.78	48	
212	104	175	280	32	.14	81	
312	186	214	300:	114	.10	90	Lightcurve inverted
122	90	164	263	18	.84	57	
222	89	172	279	17	.24	80	
322	98	178	278	26	.10	100	
132	92	164	254:	20	.84	70	
232	...	...	...	...	....	...	No data
332	68	146	251	-4	.08	110	
113	74	164	256	2	.78	43	
213	94:	200:	280:	22:	.14:	...	Peculiar
313	116:	220:	296:	44:	.08:	...	Peculiar
123	91	165	282	19	.84	51	
223	98	170	282	26	.20	73	
323	76:	160	276	4:	.08	100	
133	95	164	290	23	.82	86	
233	105	218	290	33	.24	95	
333	192	235	...	120	.06:	...	Lightcurve inverted

TABLE III. Continued Model 2

ID	Max I	Min	Max II	Time Shift	Amp. I	1/2 Width Min	Remarks
111	179°	270°	356°	0°	0.m78	81°	
211	182	276	360:	3	.30	88	
311	204	305	...*	25	.06:	...	Peculiar
121	188	275	360:	9	.82	73	
221	190	280	...	11	.38	86	
321	205	292	...	26	.14	101	
131	188	276	360:	9	.86	73	
231	188	278	360:	9	.46	88	
331	194	278	360:	15	.16	95	
112	179	270	360	0	.78	72	
212	184	278	360	5	.19	93	
312	258	350:	...	79	.10	...	Lightcurve inverting
122	194	273	...	15	.84	77	
222	206	291	...	27	.36	92	
322	214	304:	...	35	.16	98	
132	200	284	...	21	.92	83	
232	200	292	...	21	.50	91	
332	207	299	...	28	.18	...	
113	179	270	360	0	.76	65	
213	219	345:	...	40	.07	...	
313	266	352	...	87	.18	...	Lightcurve inverted
123	203	275	...	24	.88	82	
223	219	303	...	40	.40	101	
323	232	321	...	53	.20	...	
133	208	283	...	29	1.00	92	
233	211	306	...	32	.62	107	
333	219	316	...	40	.25	94	

* Max II frequently not observed

TABLE III. Continued Model 3

ID	Max I	Min	Max II	Time Shift	Amp. I	1/2 Width Min	Remarks
111	86°	177°	267°	0°	1m.66	54°	
211	88	186	268	2	.42	81	
311	150:	213	300:	64:	.10	...	Lightcurve inverting
121	93	180	276	7	1.74	53	
221	102	184	281	16	.56	78	
321	120	186	300:	34	.20	100	
131	96	184	278	10	1.80	55	
231	98	190:	279:	12	.70:	84	
331	95:	195	280:	9:	.24	110	
112	87	177	267	1	1.69	48	
212	90	192	267	4	.25	75	
312	166	258	...	80	.17	111:	Lightcurve inverted
122	100	176	282	14	1.82	59	
222	118	196	296	32	.56	98	
322	129	222	...	43	.26	123	
132	110:	186	290:	24:	1.88	70	
232	106	200	...	20	.84	90	
332	116	206	286	30	.32	102	
113	86	177	266	0	1.66	44	
213	153	207	...	67	.12	...	Lightcurve inverting
313	171	263	...	85	.30	103:	Lightcurve inverted
123	112	180	294	26	1.92	63	
223	130	212	...	44	.62	102	
323	138	231	...	52	.36	109	
133	118	186	300:	32	2.00	84	
233	117	218	300:	31	1.04	94	
333	117	230	296	31	.43	90	

TABLE III. Continued Model 4

ID	Max I	Min	Max II	Time Shift	Amp. I	1/2 Width Min	Remarks
111	78°	172°	262°	0°	0m.96	77°	
211	80	170	264	2	.46	87	
311	90:	197	290:	12:	.08	...	
121	86	174	270	8	1.00	78	
221	91	179	274	13	.58	79	
321	105	182	291	27	.20	94	
131	89	185	273	11	1.02	81	
231	90	184	273	12	.72	80	
331	92	185	276	14	.28	96	
112	78	172	263	0	1.02	72	
212	79	173	264	1	.30	84	
312	158	250	...	80	.10	...	Lightcurve inverted
122	94	188	276	16	1.16	77	
222	105	191	288	27	.56	87	
322	120	210	300:	42	.24:	103:	
132	98	194	283	20	1.32	74	
232	102	192	285	24	.86	81	
332	104	200	290	26	.36	92	
113	76	171	262	-2	.86	79	
213	100:	185	276:	22:	.11	60	Peculiar
313	160	255	...	84	.20	...	Lightcurve inverted
123	105	198	286	27	1.23	71	
223	117	201	300:	39	.56	94	
323	132	225	...	54	.28:	94:	
133	110	201	292	32	1.76	67	
233	114	204	296	36	.98	83	
333	118	214	300:	40	.42:	93	

TABLE III. Continued Model 5

ID	Max I	Min	Max II	Time Shift	Amp. I	1/2 Width Min	Remarks
					m		
111	88°	180°	272°	0°	1.56	53°	
211	87	186	276	-1	.44	88	
311	160:	216	300:	72:	.10:	...	Lightcurve inverting
121	96	180	280	8	1.60	54	
221	100	188	284	12	.60	80	
321	118	190	300:	30	.24	91	
131	97	190	283	9	1.64	59	
231	97	188	284	9	.74	83	
331	98	194	285	10	.26	96	
112	87	180	272	-1	1.58	52	
212	89	190	280	1	.30	92	
312	171	244:	...	83	.12	...	Lightcurve inverted
122	104	180	289	16	1.68	60	
222	117	195	300:	29	.59	85	
322	132	219	...	44	.26:	104	
132	108	186	292	20	1.74	71	
232	108	203	294	20	.86	93	
332	106	210	292	18	.36	98	
113	87	180	271	-1	1.60	47	
213	155:	210	300:	67:	.14	...	Lightcurve inverting
313	174	270	...	86	.28	...	Lightcurve inverted
123	115	180	300:	27	1.76	64	
223	132	210	...	44	.58:	92	
323	141	230	...	53	.38:	107	
133	118	184	300:	30	1.82	87	
233	118	216	300:	30	1.04	95	
333	117	226	300:	29	.48:	93	

TABLE III. Continued Model 6

ID	Max I	Min	Max II	Time Shift	Amp. I	1/2 Width Min	Remarks
111	90°	179°	268°	0°	1.m44	49°	
211	95	180	271	5	.48	66	
311	114:	193	288	24:	.10	72	
121	94	180	277	4	1.46	58	
221	100	182	282	10	.52	78	
321	114	180	294	24	.30	86	
131	96	183	277	6	1.48	57	
231	98	183	278	8	.72	74	
331	100	184:	282	10	.32	96	
112	90	179	270	0	1.46	50	
212	96	180	266	6	.28	69	
312	160	218	342	70	.14	107	
122	105	180	286	15	1.54	63	
222	117	184	297	27	.58	89	
322	131	183	313	41	.30	118	
132	106	180	289	16	1.56	74	
232	108	183	289	18	.74	90	
332	108	183:	289	18	.34	114	
113	88	178	266	-2	1.54	47	
213	152	208	...	62	.10	...	
313	168	219	...	78	.14	...	Lightcurve inverted
123	115	180	296	25	1.76	76	
223	131	184	...	41	.56:	114	
323	140	195	...	50	.26:	134	
133	117	179/238	300:	27	1.82	88	Double minimum
233	119	180/244	300	29	.84	104	Double minimum
333	124	178/252	300:	34	.44	118	Double minimum

TABLE III. Continued Model 7

ID	Max I	Min I	Max II	Min II	Time Shift	Amp. I	Amp II	1/2 Width Min	Remarks
111	86°	180°	272°	360°:	0°	2m.12	1m.76	51°	
211	86	186	272	360:	0	.54	.48	84:	
311	106:	210	344	23	20:	.12	.08	70	
121	91	180	278	360:	5	2.18	1.80	54:	
221	98	188	284	0	12	.68	.64	92:	
321	115	194	300	0	29	.24	.24	105	
131	90	186	280	0	4	2.28	1.78	54	
231	95	190	280	0	9	.86	.78	84	
331	95	195	278	0:	9	.30	.28	118	
112	84	180	268	360:	-2	2.24	1.82	49	
212	90	193	276	2	4	.32	.28	86	
312	166	254:	350	70:	80	.16	.14	120	Lightcurve inverted
122	102	180	286	360:	16	2.32	1.90	60	
222	116	198	298	5:	30	.68	.62	91	
322	130	222	310	30	44	.30	.28	113	
132	106	200	290	0	20	2.40	1.88	68	
232	106	200	290	10	20	1.04	.94	88	
332	106	210	290	20	20	.38	.37	100	
113	86	180	272	360:	0	2.14	1.84	48	
213	140:	210	330:	15	54:	.16	.10	120	Lightcurve inverting
313	170	265	350	80	84	.30	.30	111	Lightcurve inverted
123	112	180	296	360	26	2.34	1.96	66	
223	130	214	314	22	44	.72	.66	102	
323	137	236	321	45	51	.42	.42	110	
133	115	210	270	2	29	2.56	2.02	83	
233	116	218	300	30	30	1.28	1.12	84	
333	116	230	296	42	30	.54	.52	90	

TABLE III. Continued Model 7 continued

ID	Max I	Min	Max II	Time Shift	Amp I	Amp II	1/2 Width Min	Remarks
161	85°	179°	273°	0°	2.12 m	1.61 m	49°	
261	85	180	271	0	1.40	1.21	65	
361	85	185	271	0	.44	.40	91	
251	75	171	265	-10	1.23	1.08	70	
351	75	171	260	-10	.42	.38	88	
241	70	165	255	-15	.98	.91	76	
341	70	161	255	-15	.36	.34	90	
262	85	179	273	0	2.33	1.80	55	
362	85	181	271	0	.87	.81	80	
252	71	155	255	-14	2.29	1.80	56	
352	70	165	255	-15	.78	.72	82	
242	65	155	247	-20	1.48	1.27	74	
342	61	150	243	-24	.62	.55	84	

TABLE III. Continued Model 8

ID	Max I	Min I	Max II	Min II	Time Shift	Amp I	Amp II	1/2 Width Min	Remarks
111	78°	170°	269°	355°	0°	0m.94	0m.78	84°	
211	78	172	268	357	0	.34	.42	100	
311	76	188	300:	25	-2	.06	.10	115	
121	83	175	272	360	5	.98	.82	86	
221	90	178	280	360	12	.48	.52	90	
321	100	187	300:	4	22	.16	.22	102	
131	85	175	277	360	7	1.02	.82	91	
231	85	180	277	360:	7	.62	.60	95	
331	85	180	282	5	7	.22	.28	108	
112	78	170	265	355	0	.96	.80	83	
212	75	173	273	7	-3	.16	.33	90	
312	165	236	345	70	87	.12	.14	...	Lightcurve inverted
122	90	175	282	0:	12	1.14	.86	91	
222	97	185	297	12	19	.48	.54	98	
322	110	208	314	30	32	.20	.27	115	
132	94	173	288	9	16	1.32	.92	100	
232	92	190	290	11	14	.74	.70	102	
332	95	200	297	18	17	.26	.34	112	
113	77	170	267	355	-1	.76	.80	80	
213	...	178	342	...	...	....	.32	110	Peculiar
313	167	250	347	75	89	.18	.20	115	Lightcurve inverted
123	100	175	295	15	22	1.18	.93	97	
223	110	190	313	25	32	.50	.60	114	
323	125	220	325	45	47	.23	.31	122	
133	102	175	302	20	24	1.72	1.00	110	
233	103	200	306	23	25	.88	.78	114	
333	93	227	312	32	15	.34	.46	113	

TABLE III. Continued Model 9

ID	Max I	Min I	Max II	Min II	Time Shift	Amp I	Amp II	1/2 Width Min	Remarks
111	0°	80°	204°	300°	0°	0m.36:	0m.22	65°	
211	0	95	208	292	0	.09	.15	80	
311	...	90	270:	...	...	.01	....	...	Peculiar
121	0	80	212	308	0	.32	.22	65	
221	0	97	223	302	0	.14	.16	60	
321	5:	95	252	322	5:	.02	.06	...	
131	5	110:	220	305:	5	.30	.24	67	
231	0	100	225	300	0	.22	.18	60	
331	0:	100	240	305:	0:	.04	.08	60	
112	0	80	205	293	0	.30	.24	73	
212	343	88	220:	295	-17	.02	.15	...	
312	...	...	280:	...	...	.03	....	...	Peculiar
122	10	80	225	310	10	.46	.24	55	
222	18	100	242	312	18	.12	.18	65	
322	25	110	270	332	25	.03	.07	...	
132	10	120:	232	308	10	.50	.26	50	
232	15	100	238	310	15	.26	.22	53	
332	18	125:	250	315:	18	.06	.10	65	

TABLE III. Continued Model 10

ID	Max I	Min I	Max II	Min II	Time Shift	Amp I	Amp II	1/2 Width Min	Remarks
111	23°	112°	212°	295°	0°	0m.49	0m.41	72°	
211	23	118	202	310	0	.21	.14	75	
311	...	...	240:	...	...	.04	....	...	Peculiar
121	35	120	223	305	12	.54	.42	70	
221	25:	120	225	310	2:	.26	.18	70	
321	65	128	242	350	42	.12	.10	...	
131	35	125	218	315	12	.56	.48	...	
231	40:	125	222	310	17:	.34	.22	70	
331	45	125	226	337	22	.16	.11	90	
112	20	115	207	295	-3	.46	.38	72	
212	32	115	212	312	9	.14	.12	75	
312	110	...	298	...	87	.09	....	...	Lightcurve inverted
122	30	130	227	303	7	.52	.44	80	
222	50	123	237	315	27	.30	.24	90	
322	70	148	250	360	47	.08	.14	110	
132	45	143	225	310	22	.66	.54	78	
232	50	135	233	315	27	.42	.28	80	
332	57	140	230	340	34	.20	.17	87	

TABLE III. Continued Model 11

ID	Max I	Min I	Max II	Min II	Time Shift	Amp I	Amp II	1/2 Width Min	Remarks
111	82°	177°	268°	360°	0°	0m.82	0m.78	75°	
211	85	180	263	350	3	.24	.24	104	
311	95:	305	...	...	13:	.07	....	...	Peculiar
121	88	180	277	360	6	.86	.80	74	
221	98	190	280	0	16	.30	.30	92	
321	115	215	303	10	33	.10	.10	...	
131	90	185	278	0	8	.88	.86	75	
231	98	192	280	0	16	.40	.38	92	
331	105	203	282	5	23	.14	.15	100	
112	83	178	270	360	1	.80	.76	72	
212	90	200	250	337	8	.14	.18	...	
312	174	278	0	78	92	.10	.06	110	Lightcurve inverted
122	98	185	285	0	16	.88	.82	80	
222	112	205	300	12	30	.31	.30	102	
322	135	237	320	35	53	.14	.14	118	
132	103	195	290	15	21	.98	.96	84	
232	110	208	295	15	28	.48	.48	94	
332	117	220	295	22	35	.19	.24	95	

TABLE III. Continued Model 12

ID	Max I	Min I	Max II	Min II	Time Shift	Amp I	Amp II	1/2 Width Min	Remarks
111	108°	195°	273°	15°*	0°	0m.62	0m.46	60°	
211	112	178	265	360	4	.12	.20	80	
311	222	10	...	...	14	.08	....	...	Peculiar
121	115	198	282	20 *	7	.80	.46	54	
221	125	198	280	5	17	.20	.24	76	
321	140	220	285	8	32	.06	.12	...	
131	115	198	292	35 *	7	1.00	.54	49	
231	120	198	280	5	12	.32	.30	82	
331	127	208	280	15	19	.13	.18	...	
112	108	198	276	18	0	.60	.50	60	
212	122	165	250	5	14	.04	.16	...	
312	190	298	360	95	82	.08	.10	...	Lightcurve inverted
122	120	200	285	355 *	12	.96	.52	54	
222	138	217	295	0 *	30	.23	.24	87	
322	150	253	312	65 *	42	.12	.16	100	
132	125	205	287	58 *	17	1.18	.66	56	
232	130	217	290	48 *	22	.42	.34	76	
332	132	230	292	48 *	24	.18	.22	88	

* Min II is double — deeper minimum is given in table

Fig. 4 illustrates 27 lightcurves obtained with model 7. The amplitude of the lightcurve in the upper left corner (aspect 90°, obliquity 90°, phase 20°) is $2^{m}.12$. Several characteristics of the lightcurves can be identified that are used later in making comparisons of the models:

1) Amplitude: the height of the curve from minimum to maximum.

2) Shape of minima: sharp, flat and/or asymmetric.

3) Width of minima at half amplitude.

4) Time-shifts of the maxima (or minima) relative to the observation at 90° aspect, 90° obliquity, 20° phase.

5) Lightcurve inversion: maxima become minima and vice versa; (time-shift is ~90°).

6) Primary and secondary maxima and minima.

Looking horizontally from left to right in Fig. 4, one sees the change produced by decreasing the aspect. Most noticeable are the decreases in amplitude and the time-shifts (leading to two lightcurve inversions and two partial inversions at the top right of the figure. The inversions are understood qualitatively as occurring when the illuminated part of the "true" maximum has a smaller area (as seen by the detector) than the illuminated part of the "true" minimum. Looking vertically, one sees the changes produced by changing the obliquity. Sometimes there is a marked change in amplitude and sometimes there are changes in the shape of the minima. Looking diagonally (in groups of three), one sees the changes due to phase. These are usually small changes in amplitude with some changes in the shape of the minima and in time-shifts. Usually an increase in the phase angle enhances any peculiarity noted at a smaller phase.

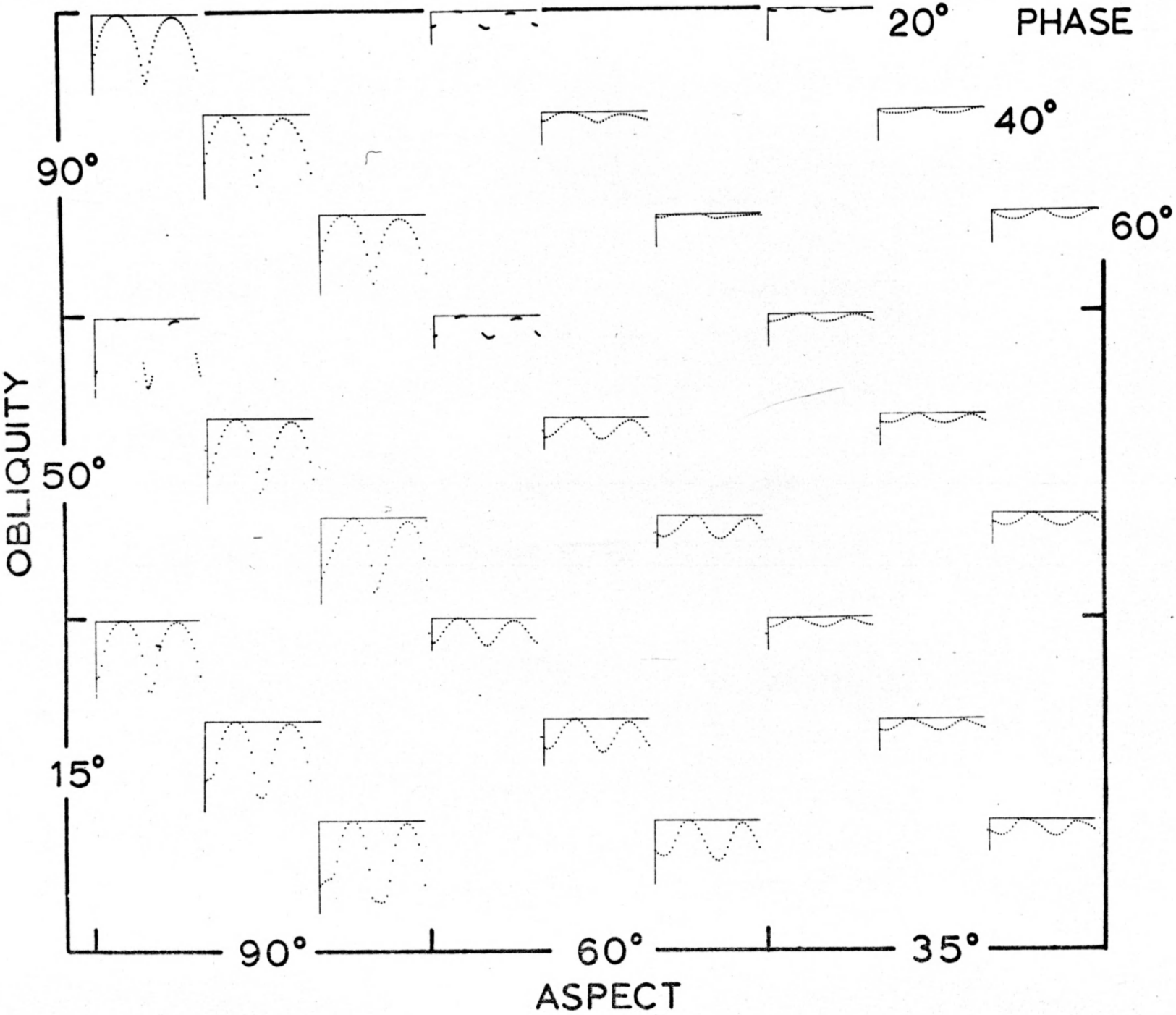

Fig. 4. Lightcurves of model 7. The one at the top left has an amplitude of $2^{m}.12$.

IV. ANALYSIS OF THE MODEL LIGHTCURVES

Nearly all the lightcurves generated in this study had two maxima and two minima. The average difference between the two maxima was generally small, less than $0^m.04$, for all models except 7, 8, and 12, for which the average difference was about twice as great. Each of these models had visable differences between their opposite sides: model 7 was darkened with graphite on one side more than the other, model 8 had some patches of dust that had not completely darkened by the time it was run (cf Fig. 2, second model from right), and model 12 had a large chunk cut from one side (see sketch in Table II). Occasionally with model 8 the primary and secondary minima were reversed. This happened only at the smallest aspect and was therefore mostly due to the peculiar shape of the ends (one rounded, the other conical) rather than the spotty surface. Aside from these three unusual models, the small average difference between the lightcurve maxima indicates that the model surfaces had small reflectivity differences and, in fact, agreed with the difference found by Van Houten for lightcurves whose amplitudes were $>0^m.2$ (Sec. I). However, the model lightcurves were much smoother than most asteroid lightcurves, even for models 5 and 10 which had irregular bumps on their surfaces. For comparison, a few lightcurves were made of a very irregular piece of bare coke-like rock with a pyroclastic texture, dark grey color, and numerous glassy surfaces less than 1/4 mm^2 in area. The size of the rock was similar to the less elongated models. Its lightcurves were the only ones that were not definitely smooth, but showed small fluctuations within 5° - 15° of rotation. More work needs to be done on modeling the surface texture, although the models studied

in this investigation suggest that an irregular shape is not sufficient to account for the small deviations from smoothness seen in many asteroid lightcurves.

A. Amplitude - Aspect Relationships

The most obvious change in the model lightcurves is the change in amplitude with aspect (cf Fig. 4). This is not new - it was recognized early in the analysis of the telescopic observations of Eros and was used by several authors to determine the pole and later the shape of Eros (see Vesely 1971 for a review). Other writers have used amplitude-aspect functions to determine the poles for several asteroids. Fig. 5 is the set of the nine amplitude-aspect relations for the lightcurves of Fig. 4 (using secondary amplitudes to avoid reflectivity effects). Curves for the other models are similar, but not exactly the same as these. The rise in the curves at 90° obliquity and 40° and 60° phase is associated with lightcurve inversions. It is clear that there is no unique amplitude-aspect function for this or any of the models studied. Therefore, it is not possible, in general, to determine a rotation axis precisely by using a function that depends only on amplitude and aspect.

Most asteroids are observed at phase angles $< 20^{\circ}$. It is noted in Fig. 5 that the spread of the relations is considerably reduced if we consider only the observations at 20° phase (solid lines). Fig. 6 illustrates the relations at 20° phase for the first 12 models. With some exceptions (especially models 4 and 8), most of the differences in these relations are due to the elongation of the models rather than their particular shapes. Consequently, if a particular asteroid has lightcurves that closely resemble those of

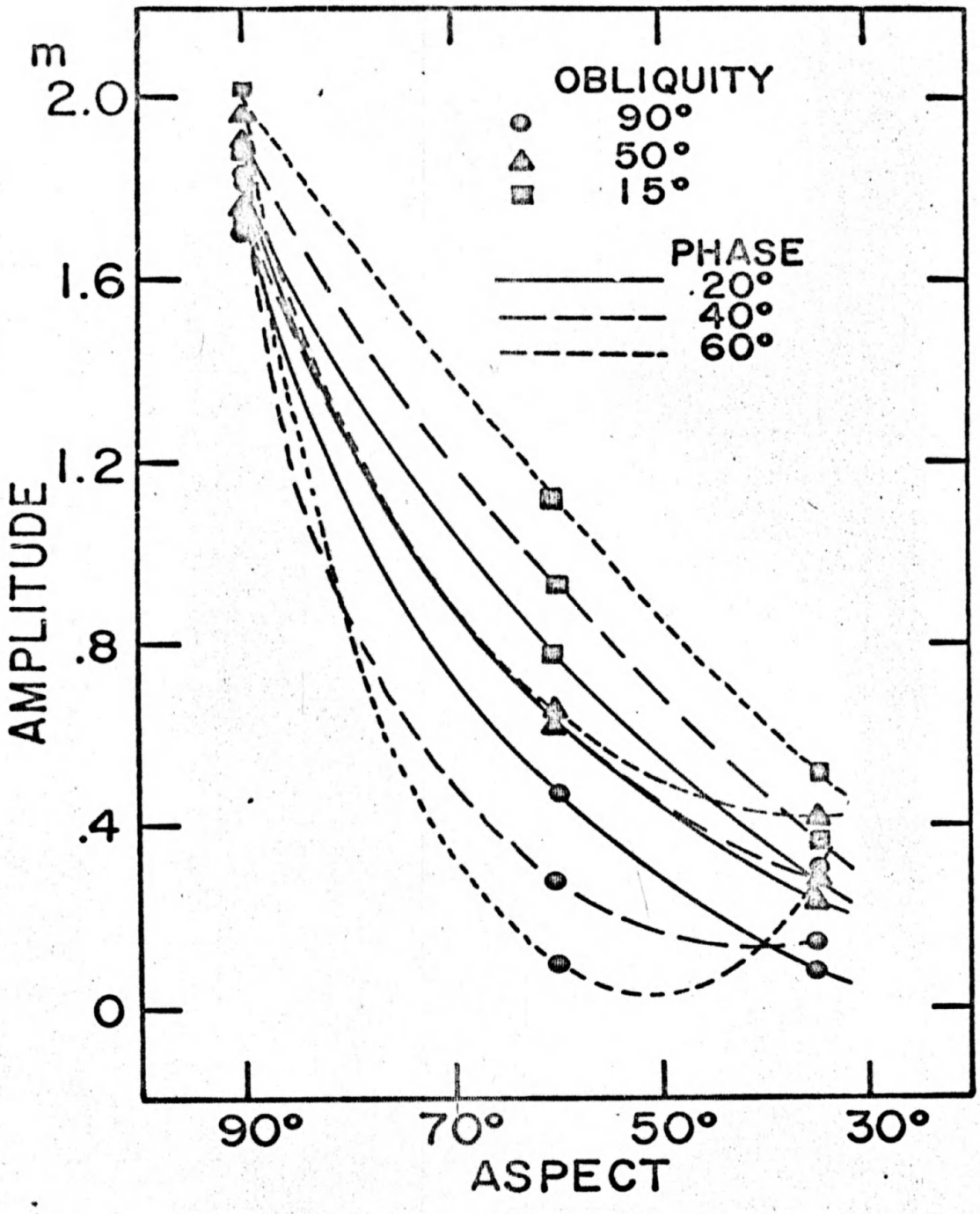

Fig. 5. Amplitude-aspect curves obtained from the secondary amplitudes of Fig. 3.

Fig. 6. Amplitude-aspect curves at 20° phase for models 1 - 12. Symbols for different obliquity are the same as Fig. 5.

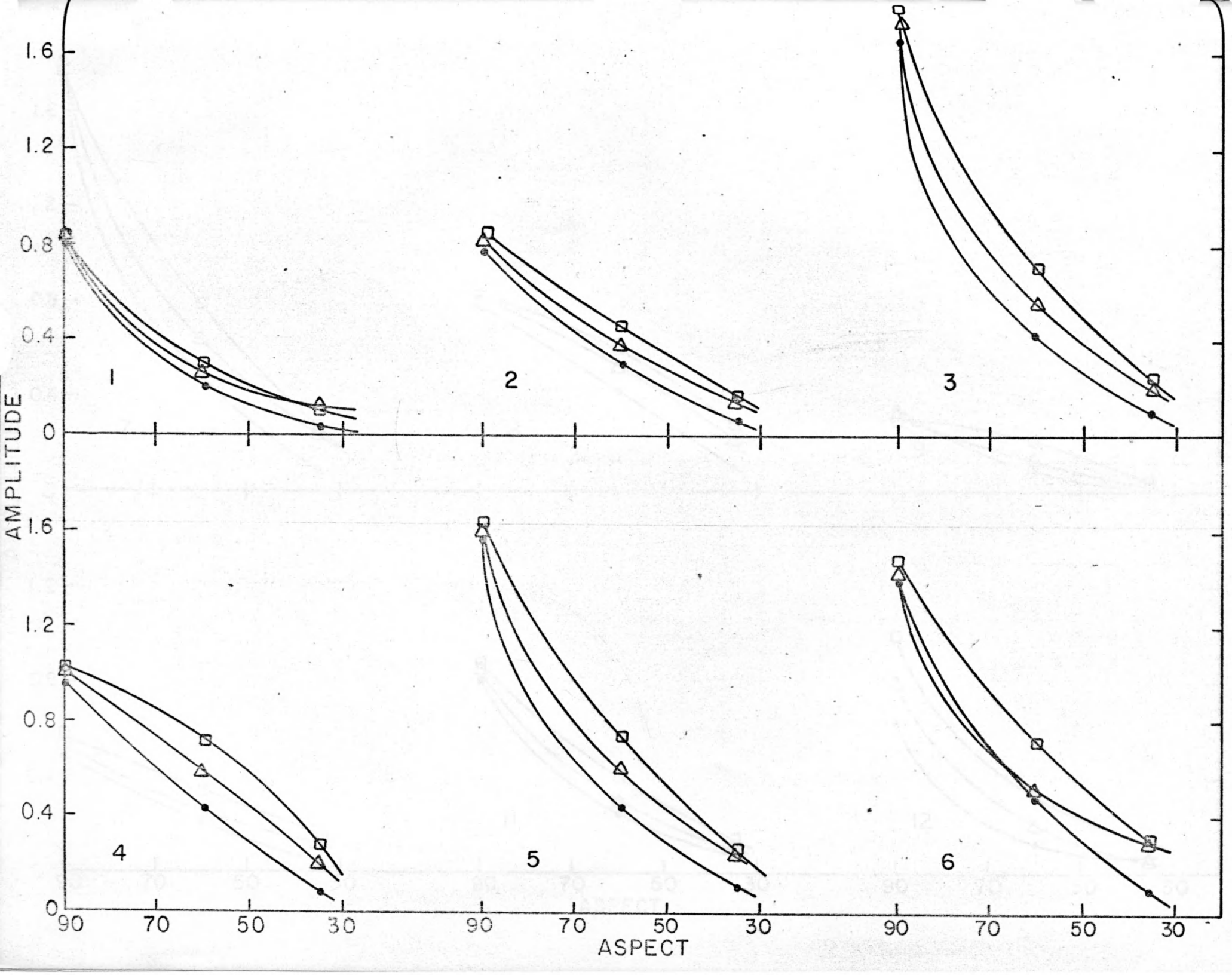
1.6
1.2
0.8
0.4
0
AMPLITUDE
1
2
3
4
5
6
90
70
50
30
ASPECT

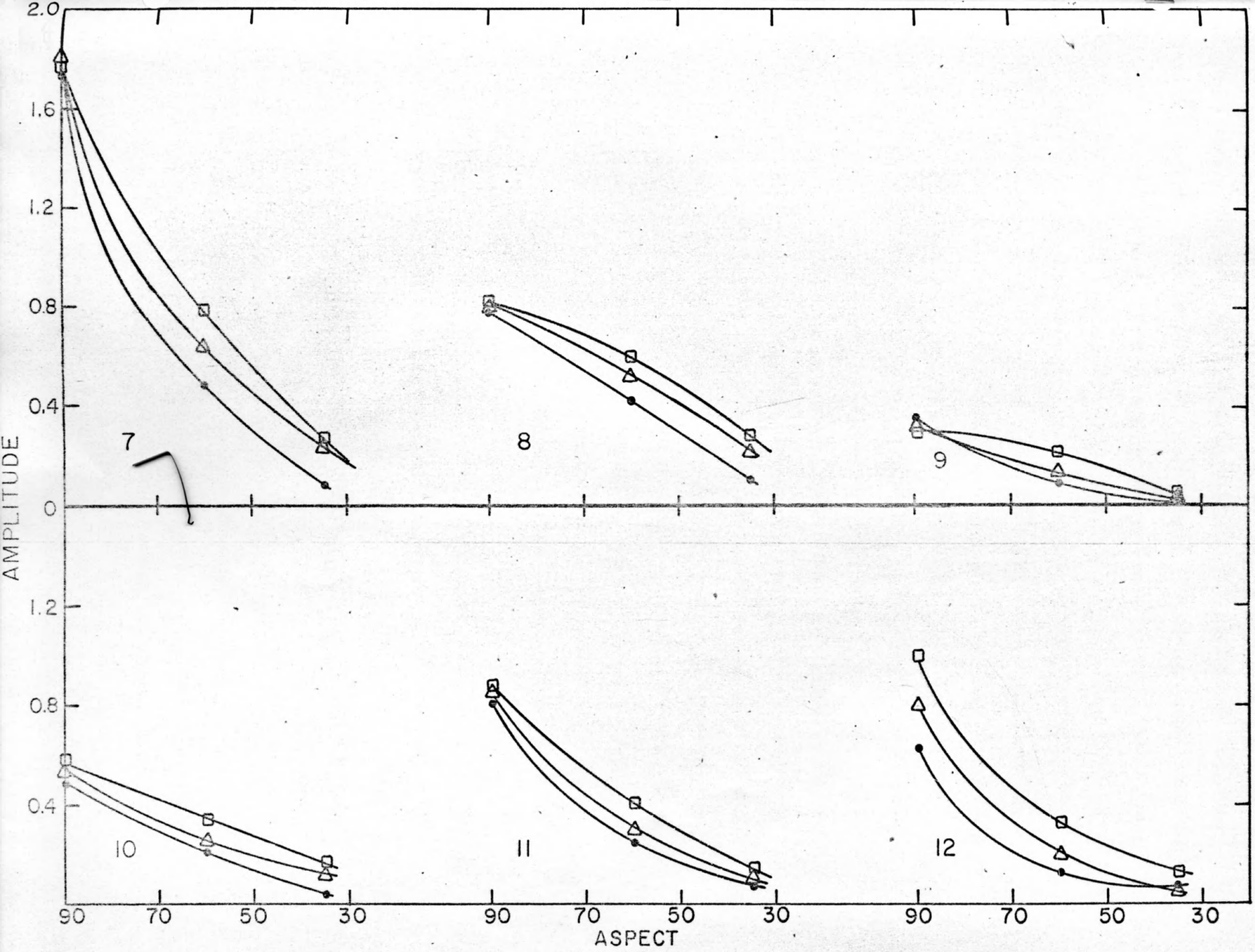
2.0
1.6
1.2
0.8
0.4
0
AMPLITUDE
7
8
9
1.2
0.8
0.4
10
11
12
90
70
50
30
ASPECT

the models, then an amplitude-aspect relation may be used to obtain an approximate orientation of the axis of rotation. Fig. 7 illustrates a family of amplitude-aspect functions derived from the model curves of Fig. 6. The curves were obtained by plotting the amplitudes of all the models for a constant aspect and an average obliquity as a function of log A max/A min, the ratio of the maximum area of cross-section to the minimum area of cross-section. This was done for each of the three observed aspects. For each aspect, the points were fitted to a straight line. Models 4 and 8 deviated most from this line ($\lesssim 0\overset{m}{.}2$), whereas the average deviation of the other points was $\pm\ 0\overset{m}{.}04$. In addition, if one considers the range in amplitudes caused by the various obliquities, the average deviations are increased further to about $\pm\ 0\overset{m}{.}07$, being largest at 60° aspect, and smallest at 35° aspect. This means that the lines in Fig. 7 should be considered as central tendencies with an average width of about $0\overset{m}{.}14$. An example of how one could use these curves to obtain an estimate of the position of the rotation axis of an asteroid will be given in Sec. V A. Unfortunately, most large belt asteroids have relatively small amplitudes, and the usefulness of this approximate method is severely limited. All asteroids whose maximum observed amplitudes exceed $1\overset{m}{.}0$ (Eros, Geographos, 1971 FA, and Hektor) have unusual orbits. Only Hektor, a Trojan, is always observed at phase angles less than 20°. The anticipated probable error in the determination of an axis of rotation using the above method for suitable observations when the phase angle is less than 20° is about $\pm\ 10^{\circ}$ in longitude and latitude. This error increases rapidly at larger phase angles, primarily due to the effect of the unknown obliquity. Sec. V B discusses a technique for obtaining an approximate rotation

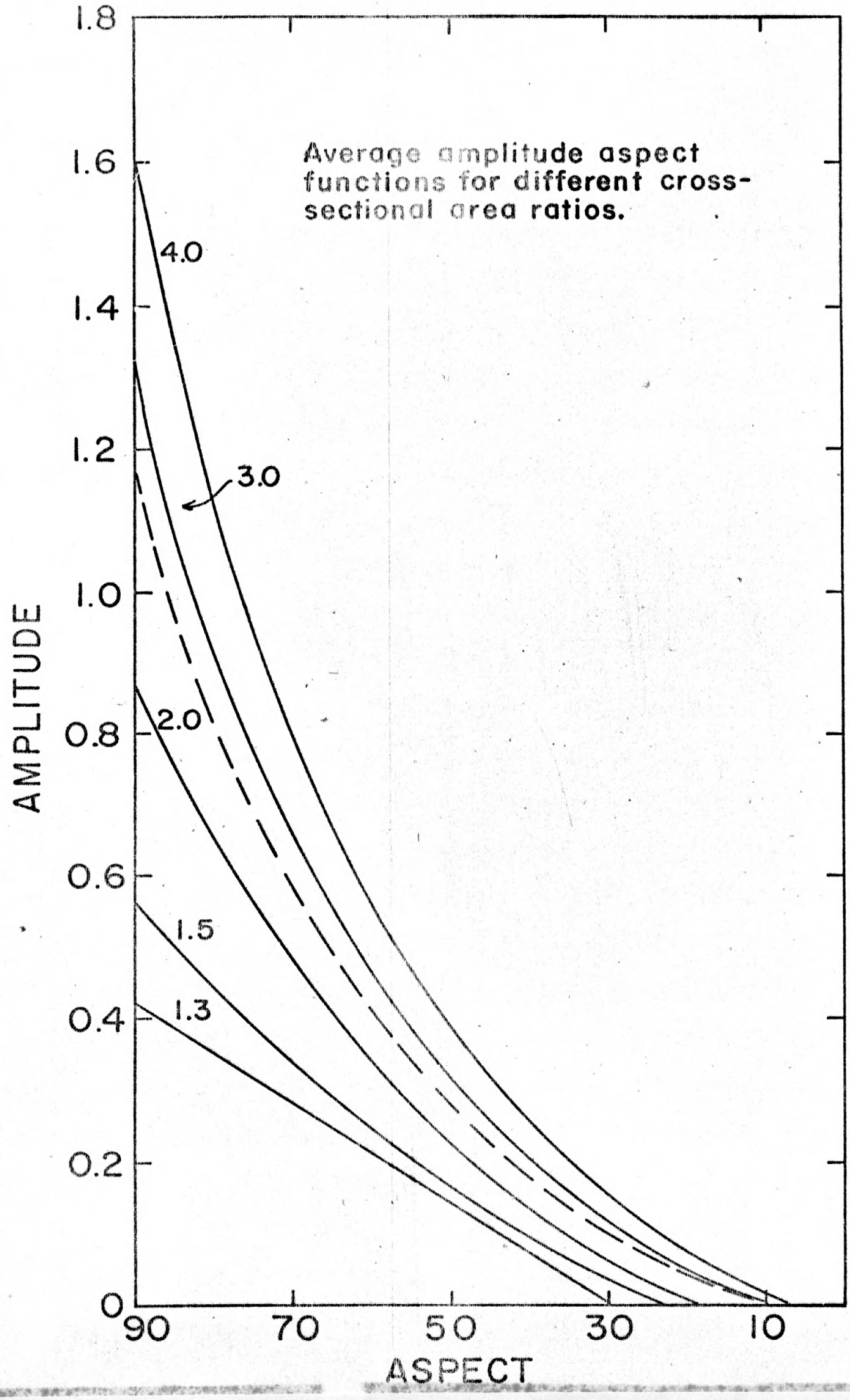

Fig. 7. Average amplitude-aspect functions from Fig. 6.

axis in such cases.

B. Comparison of Models

Table IV is a summary of intercomparisons of lightcurves of several models. In the first column, the models are described by indicating the difference with the reference model, which in each case is a cylinder with hemispherical ends and a cross-sectional area ratio of 1.9. The remaining columns give the observed differences in the lightcurves relative to the reference model's lightcurves. It should be noted that these changes usually depend on the aspect, phase, and obliquity, and do not characterize all the lightcurves. Important conclusions from this table are:

1) The more elongated the asteroid, the larger the amplitude and the narrower the minima.
2) If the asteroid is elongated in two dimensions (i.e., a 3-axis ellipsoid), the minima are somewhat wider, but perhaps more important is the increase in brightness of the maxima as aspect decreases.
3) If the ends are tapered rather than blunt, lightcurves at large aspect and obliquity have wedge-shaped minima.

Not included in the table are the lightcurves of model 10 which was given a peculiar cratered surface. Several, but not all, of its lightcurves show a tertiary feature - an extra bump in between a normal maximum and minimum. The bumps were most conspicuous at an intermediate aspect. However, the overall behavior of amplitude as a function of aspect was not much different from the other models, except at small aspects where the amplitude was about two times larger than average.

TABLE IV. INTERCOMPARISONS OF MODELS

OBSERVED CHANGES IN LIGHT VARIATION RELATIVE TO THE REFERENCE MODEL†

MODELS COMPARED WITH REFERENCE *	AMPLITUDE	SHAPE OF MINIMA	TIME-SHIFTS	OTHER
1. Same shape, but cross-sectional area ratio 2.3 times larger.	Larger by up to a factor of 2.	Narrower, sharper, more asymmetry.	Some larger shifts in maxima.	Lightcurve inversion is possible at smaller phase angle.
2. Two tangent spheres of equal radii and 5% larger area ratio.	Usually smaller.	Narrower, sharper.	Some smaller shifts in maxima, more in minima.	--
3. Both ends pointed (conical) and ∿ 5% larger area ratio.	Somewhat larger. Amplitude-aspect curves have less or opposite curvature.	Complicated changes with less asymmetry.	No significant change.	Occasionally the minima are wedge-shaped.
4. One end pointed (conical) and some brighter spots and 5% smaller area ratio.	Primary and secondary amplitudes larger, except at 90° aspect.	Wider minima with one resembling the reference and the other those of 3 (above).	Some smaller shifts in maxima and minima.	Primary and secondary minima are frequently interchanged.
5. Elongation along a second body axis 0.7 times the major axis. 3% larger area ratio at 90° aspect.	Smaller, except at 90° aspect.	Somewhat wider.	Usually larger shifts in maxima and minima.	Increase in brightness of the maxima as aspect decreases (up to $0^m.32$ at 35° aspect).

* The reference model is a cylinder with hemispherical ends and a cross-sectional area ratio, $\frac{A_{max}}{A_{min}}$, of 1.9.

† These changes usually depend on the aspect, phase, and obliquity and therefore do not characterize all the lightcurves.

Also omitted from the table is the occasional appearance of a wide double minimum in some equatorial lightcurves of models 6 and 12. The effect is more pronounced at large phase angles and small obliquities and is related to the flat surfaces these models possess.

One goal of this study was to identify characteristics in the lightcurves which could be attributed to the shape of the object. In general this is not possible until a precise axis of rotation is known, and even then the answer may not be unique. To illustrate what can be done at this point, consider a typical situation in which we are given a set of lightcurves of a particular asteroid obtained in at least three different oppositions which are uniformly distributed in ecliptic longitude. Suppose that in addition, there are two maxima at about the same level and two minima at about the same level on each lightcurve, the amplitude varies with longitude and has a maximum of at least $0^m.4$, the phase angles are about 20° or less, and tertiary features are absent or very small ($\sim 0^m.04$). Under these conditions, the following conclusions seem justified.

1) The lightcurves are shape dominated.
2) Amplitude-aspect may give an approximate pole.
3) The elongation is primarily along one axis if the maxima have about the same absolute magnitude.
4) The elongation is unequal along three perpendicular axes if the maxima have different absolute magnitudes.
5) Bumps or holes on the surface have a size $< 20\%$ of the object's smallest diameter.

Two classes of "simple" shapes for which amplitude-aspect would give an erroneous pole are a double body, and an object with

tapered ends. It does not seem possible to clearly identify these shapes from lightcurves at small phase angles unless the pole is known a priori, and an observation at about 90° aspect exists. Chances are better at larger phase angles, but the pole still needs to be known first. This is a vicious circle unless there is another method of getting the pole (Sec. V). If the pole can be so determined, then the distinction between these two shapes is in the shape of the minima when the aspect is 90°. A double body gives very narrow sharp minima, whereas the object with tapered ends has wider minima which may even appear wedge-shaped. Similarly, if the pole is known, the distinction between a double body and a single body with rounded ends or tapered ends lies in the shape of the amplitude-aspect relations, or in some cases (again, near-equatorial aspects), in the shape of the minima.

Clearly the crucial problem is to find a method of determining the rotation axis with high precision (up to $\pm$ 1° for an extremely elongated object) before any details of the shape can be established.

V. COMPARISON WITH TELESCOPIC OBSERVATIONS

One test of a model lies in its ability to explain previously known phenomena. However, finding a suitable asteroid for comparison is not easy. Their shapes are unknown, and the computed rotation axes vary depending on who made the determination (cf. Vesely 1971). According to the classification in Sec. I, there are eight candidates for comparison. Half of these have published values for a rotation axis. Two of these were chosen for comparison: (624) Hektor, and (1620) Geographos, the latter for which some of the models were actually constructed. In the case of Geographos, it would not have

been possible to obtain the rotation axis without the model data.

A. (624) Hektor

The published position of the North Pole of Hektor is (324°, 10°) ecliptic longitude and latitude, respectively (Dunlap and Gehrels, 1969). Since all the observations were made at 6° phase or less, and there was a dramatic change in amplitude with longitude, the comparison will be made by using the average amplitude-aspect relations from the models to derive a pole, and to see if a particular shape for Hektor can be identified.

The near constant value of the absolute magnitude of the lightcurve maxima at all oppositions indicates that the elongation is primarily along one axis. The maximum possible amplitude appears to be about $1\overset{m}{.}2$. Consequently an interpolated amplitude-aspect function was drawn as a dotted line on Fig. 7 and used to obtain the aspect for each of the Hektor observations. Table V lists the observations and the aspects obtained. (Aspect', in the last column, will be explained later.) Each observation was located (in ecliptic coordinates) on a sphere. Then small circles were constructed about each observation point with radii equal to the aspect angle for each observation. The intersection of these circles gives the longitude and latitude of the pole. All small circles intersected near (305°, 25°) except the 1957 observations, which were close to the opposite pole of (125°, -25°). Allowing for the estimated error claimed for this method ($\pm 10^{\circ}$), this is in fairly good agreement with the published pole. Therefore, the lightcurve of 29 April 1968 is adopted as nearly equatorial and we look for a clue regarding the shape. For this position of the pole, the obliquity

TABLE V. OBSERVATIONS OF HEKTOR

Date U.T.	Ecliptic Long.	Lat.	Amp.	Aspect	Astrocentric* Long.	Lat.	Aspect'
57.05.05	249°.5	-22°.1	m.800	79°	69°.5	+22°.1	82°
57.05.31	246.1	-22.6	.775	78	66.1	+22.6	81
65.02.04	119.4	+14.7	.113	33	299.4	-14.7	39
67.03.07	193.0	- 9.9	.398	59	13.0	+ 9.9	64
68.04.29	226.2	-20.2	1.088	87.5	46.2	+20.2	88.5
68.05.01	225.9	-20.3	1.055	86.5	45.9	+20.3	87.5

* On Hektor

on this date was small. The lightcurve minima are very sharp, which tends to rule out the possibility of tapered ends. The half-width of the minimum is 50°. Although there is no model with the proper elongation for a direct comparison, the elongation lies about halfway between models 2 and 3, and perhaps a little closer to 2. Simply averaging their half-widths gives 64° at 20° phase, but this is reduced to 55° at 4° phase. This is about what the model of Dunlap and Gehrels would predict, since models 2 and 3 are cylindrical with hemispherical caps. The half-width of the double body (model 1) is 52° when corrected for phase. But model 1 does not have sufficient elongation to produce a $1^{m}.2$ lightcurve amplitude. If it is elongated by assuming that the region between the two spheres is sufficiently filled in with material (in this case, the spheres could not be tangent), or the two bodies are ellipsoidal with their long axes colinear, then sufficient amplitude could be obtained. Since elongating a model tends to reduce the half-width, the expected half-width of such an object could be less than 52°, which approaches the observed value of 50°. This is an interesting conclusion in view of the suggestion that Hektor may be a binary asteroid (Cook, 1971).

If Hektor is a double body, then the amplitude-aspect relations used above are incorrect, which means a different pole could be derived if a proper amplitude-aspect function for a double body was available. An approximate function was constructed, and the resulting aspects are listed in the last column of Table V. The corresponding pole is at (300°, 30°). This illustrates the sort of error introduced by using a different amplitude-aspect function than the curves of Fig. 7.

It is of interest to note that this method also gives a solution near (150°, 50°). This pole would have an obliquity near 90° on 29 April, for which the phase corrected half-widths are about 70° and 50° for the cylindrical and double body, respectively. Now only the double body comes close to reproducing the observed half-width. There does not seem to be any reason for preferring one solution for the pole over the other as determined by this method. Dunlap and Gehrels adopted the former pole, but their Table VII (p. 802) shows that there may be another solution near (165°, 15°). The major difference between the model solutions and their solutions is in the latitude of the pole. It has been noted (Vesely, 1971) that some amplitude-aspect methods tend to give high latitudes. This occurs when the amplitude-aspect function approaches zero amplitude at large aspect. As Fig. 7 clearly shows, one cannot take the slope of a function with large maximum amplitude and apply it to a case of small maximum amplitude - the slope changes with the elongation and isn't a constant anyway. However, this is not a likely explanation for the high latitude of the Hektor pole found here, unless the actual amplitude-aspect relation is more nearly linear than the model data would suggest, or that there is an undetermined variation in amplitude with obliquity.

In summarizing the comparison of the model data with the observations of Hektor, it appears that the use of an approximate amplitude-aspect relation can give an approximate solution for the rotation axis, and that the model data suggests that Hektor may be a double body rather than a cylinder with rounded or tapered ends, although further model work may be necessary to verify this shape due to the uncertain extrapolation of the 1/2 width of the double-sphere model.

B. (1620) Geographos

The observations of Geographos in 1969 during a close approach to Earth resulted in lightcurves having up to $2^{m}.0$ amplitude and ranging in phase from 20° - 60° (Dunlap, 1972). These observations stimulated the model study to see what shape would reproduce in the laboratory the observed lightcurves. Initially the axis of rotation of Geographos was obtained in the usual manner (Taylor, 1971) resulting in a pole of (113°, 84°) ecliptic longitude and latitude respectively. One of the models (# 7) was specifically built to reproduce the essential features of the lightcurve of 31 August 1969. It was a cylinder with rounded ends and was darkened with graphite powder on one end and part of one side to reproduce the primary minimum and the secondary maximum. (The elongation is primarily along one axis as noted by the nearly constant value of the absolute magnitude of the primary maxima.) Having the position of the pole, laboratory coordinates were computed for the observed lightcurve, and the model lightcurves closest to this orientation were interpolated to find a model lightcurve for comparison. Fig. 8 shows this comparison with filled circles for the observations and open circles for the model. While the amplitudes are fairly well matched, the width and shape of the minima do not agree. Inspecting the lightcurves of the other elongated models at this orientation revealed that none were narrow and sharp; therefore, it was difficult to imagine a simple model that would produce the desired lightcurves at this orientation. Consequently, the position of the rotation axis became suspect, and the usual method for obtaining the pole was questioned. In particular, one problem was the method by which

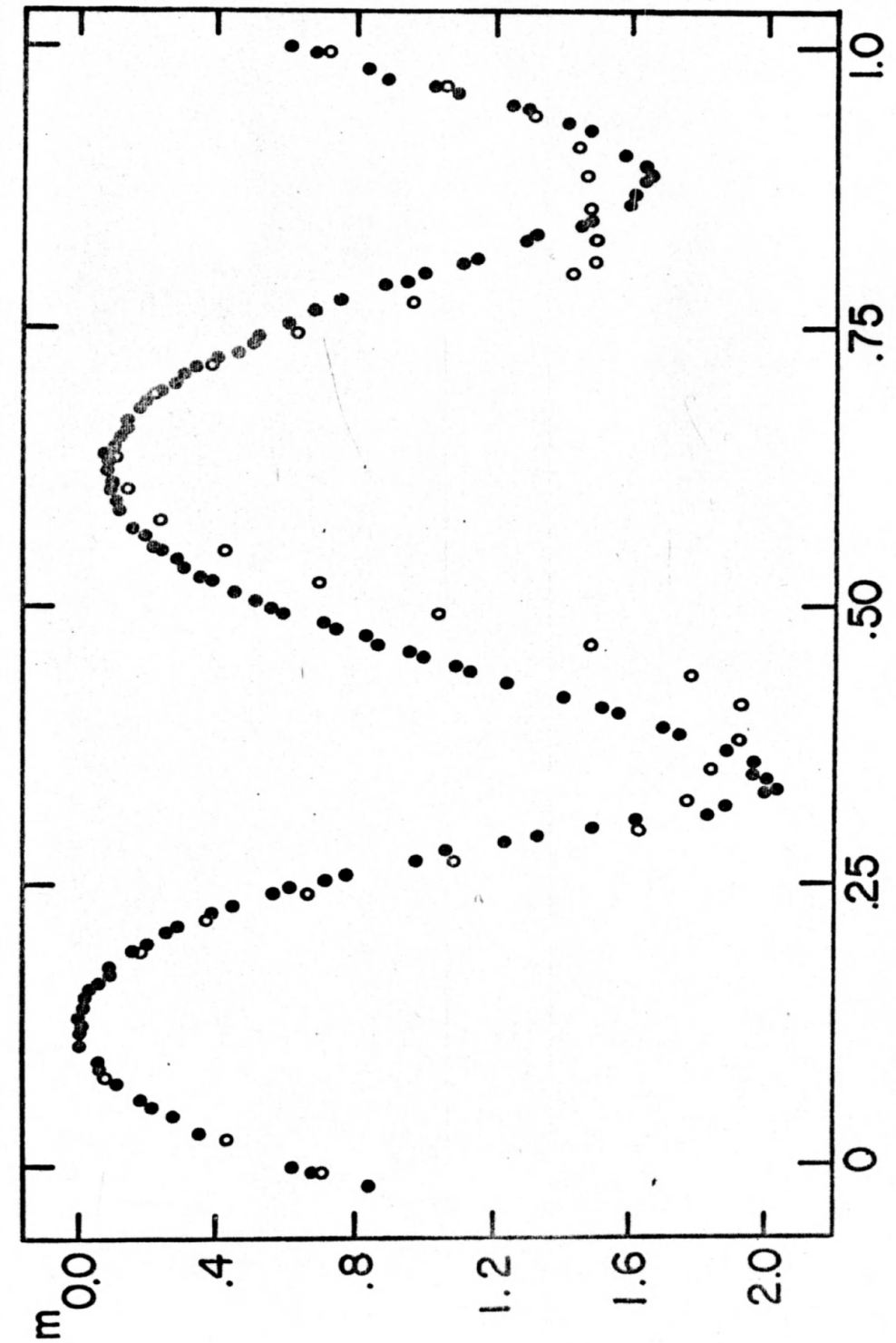

Fig. 8. Geographos lightcurve (31 Aug. 1969) and model 7 comparison; pole at (113°, 84°) ecliptic longitude and latitude, respectively.

a light center was defined and used to obtain a differential correction for phase. A spherical approximation seemed inappropriate for an elongated body. It was determined that when no differential phase correction was used, the resulting pole was shifted 70^{o} in longitude from the first solution. Furthermore, if the first solution for the pole was no good, then the elongation of the model could be wrong also. Because of the large phase angles, the simple amplitude-aspect method of getting an approximate pole is too unreliable. It was decided in this case that an approximate pole could be found from the model 7 amplitude data by a trial and error method of trying various coordinates for the pole, calculating the resulting laboratory coordinates of each observation, and then interpolating in the model amplitude data to find a model amplitude corresponding to each observation. The pole should be close to the position for which the observed amplitudes minus the model amplitudes is either least, or small and nearly constant, which would indicate that either a longer or shorter model would suffice, depending on the sign of the difference.

The following procedure was used to compute the laboratory coordinates. The phase angle was obtained from the observations in the usual manner. Only the magnitude of the phase angle is important in this case. Fig. 9 shows the asteroid sphere in an ecliptic longitude and latitude reference frame. (The asteroid may be pictured as circumscribed by the sphere, although this is not important in the derivations.) The sub-earth point, EP = (λ_e, β_e), and the sub-solar point, SP = (λ_s, β_s), are found in ecliptic coordinates as follows.

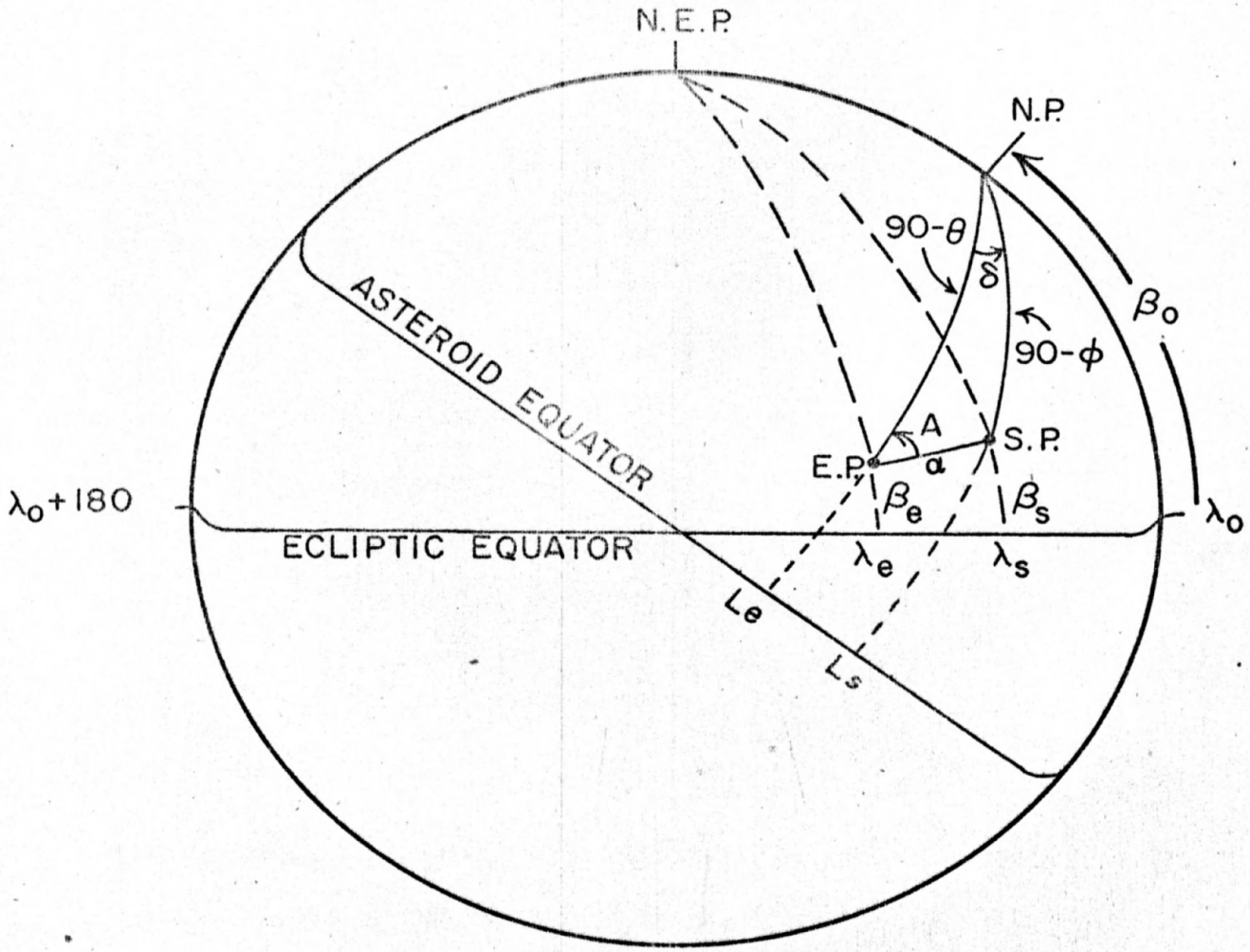

Fig. 9. Asteroid sphere and laboratory coordinates.

Let

λ_a = ecliptic longitude of asteroid

β_a = ecliptic latitude of asteroid

$\lambda_\odot$ = ecliptic longitude of Sun

R = heliocentric distance of Earth (a.u.)

Δ = geocentric distance of asteroid (a.u.)

Then for the sub-earth point,

$$\lambda_e = \lambda_a + 180^\circ \tag{1}$$

$$\beta_e = -\beta_a \tag{2}$$

and for the sub-solar point,

$$\lambda_s = \lambda_\odot \pm \text{Arc cos} \left[\frac{R - \Delta \cos \beta_a \cos (\lambda_a - \lambda_\odot)}{\sqrt{X}}\right] \tag{3}$$

Use + when $-180 < (\lambda_a - \lambda_\odot) < 0$

or when $(\lambda_a - \lambda_\odot) > 180$

Use − when $0 < (\lambda_a - \lambda_\odot) < 180$

or when $(\lambda_a - \lambda_\odot) < -180$

$$\beta_s = - \text{Arc tan}\left[\frac{\Delta \sin \beta_a}{\sqrt{X}}\right] \tag{4}$$

where $X = R^2 + \Delta^2 \cos^2 \beta_a - 2\Delta R \cos \beta_a \cos (\lambda_a - \lambda_\odot)$ (5)

The phase angle α along with the above ecliptic coordinates of the sub-earth and sub-solar point are used to obtain the aspect and obliquity of each observation for each trial value of the pole (λ_o, β_o) as follows.

The aspect is $90 - |\Theta|$, where

$$\sin \Theta = \sin \beta_e \sin \beta_o + \cos \beta_e \cos \beta_o \cos (\lambda_o - \lambda_e) \tag{6}$$

where $-90 \leq \Theta \leq 90$.

The obliquity is $90 - A$, where

$$\tan A/2 = \left[\frac{\sin (S - \alpha) \sin (S - \beta)}{\sin (S - E) \sin S}\right]^{1/2}, \text{ where } \beta = 90 - \Theta, \tag{7}$$

$S = 1/2\ (\alpha + \beta + E)$, $E = 90 - \phi$, and $0^\circ \leq A \leq 180^\circ$

and

$$\sin \phi = \sin \beta_s \sin \beta_o + \cos \beta_s \cos \beta_o \cos (\lambda_o - \lambda_s) \qquad (8)$$

where $-90 \leq \phi \leq 90$.

Although Fig. 9 reveals that angle A could actually have any value from 0° - 360°, the design of the apparatus limited the model observations to the first and third quadrants for A. Consequently, the assumption was made that the model lightcurve amplitude for angle A would be the same as that for angle 360° - A. A quick inspection of this situation suggests that the assumption is reasonable if the asteroid has a fairly uniform surface, especially on its ends. What is changed if A exceeds 180° is the sense of the asymmetry of the minima and the sign of the time-shift. The former is related to the sense of rotation. The latter's sign can be determined by comparing the astrocentric longitudes of the sub-earth point and sub-solar point. (See p. 53.)

Having now obtained the laboratory coordinates of each observation for each trial position of the North Pole, an amplitude was obtained for each observation by a triple interpolation of the model amplitudes to these coordinates. This model amplitude was then compared to the observed lightcurve amplitude and a position of the pole was found which gave the minimum residuals for all observations.

The assumed value of the North Pole was allowed to vary in 20° increments from 0° - 360° in ecliptic longitude and in 15° increments from 0° - 90° in ecliptic latitude. The computations were made on the IBM 1130 computer, and were actually made for four Geographos observations. Table VI lists these observations by

TABLE VI. OBSERVATIONS OF GEOGRAPHOS

Date U.T.	E.P. λ_e	E.P. β_e	S.P. λ_s	S.P. β_s	Phase	Amp.
69.01.09	$283^{\circ}.6$	$-27^{\circ}.4$	$287^{\circ}.0$	$-10^{\circ}.3$	17°	$1^{m}.10$
69.08.31	101.5	+ 9.9	154.4	+ 0.6	53	1.66
69.09.03	112.6	- 0.1	157.0	0.0	44	1.56
69.10.07	147.5	-21.9	183.0	- 5.9	38	1.60

date, and includes the EP, SP, phase, and amplitude of the light-curves. Refer to Table II for the complete set of observations of model 7. Secondary amplitudes were used assuming that some darkening mechanism produced the deep primary minima. The result of this amplitude comparison indicated that a minimum residual amplitude $\pm$ $0^m.09$ did occur for a pole of (100°, 82°) which is close to the earlier solution, but a somewhatsmaller residual was obtained near (200°, 60°) for which the model amplitudes were systematically too large by about $0^m.10 \pm 0^m.04$.

To try to distinguish between these possibilities, further laboratory work was done using models 5, 7, 13 and 14. In this test, models 5 and 7 were observed at the laboratory coordinates for the dates in Table VI assuming the pole was at (113°, 84°). Models 13 and 14 were especially built to give about the right secondary amplitudes if the pole was at (200°, 60°), and these models were observed at the laboratory coordinates for this pole for the four observations in Table VI. Fig. 10 illustrates the quality of the fit of the model 13 and 14 lightcurves to the 31 August 1969 Geographos lightcurve. The fit of these models to the other observations was quite similar. However, models 5 and 7 consistently had wider lightcurve minima than the Geographos lightcurves (cf. Fig. 8). Consequently, both the amplitude and shape of the Geographos lightcurves are consistent with a pole near (200°, 60°) as determined from the model data. This casts further doubt on the "routine" method of finding the pole by determining precise lightcurve epochs, applying a phase correction, and solving for a unique sidereal period and pole. In the case of the Geographos data, the phase correction could be a source of

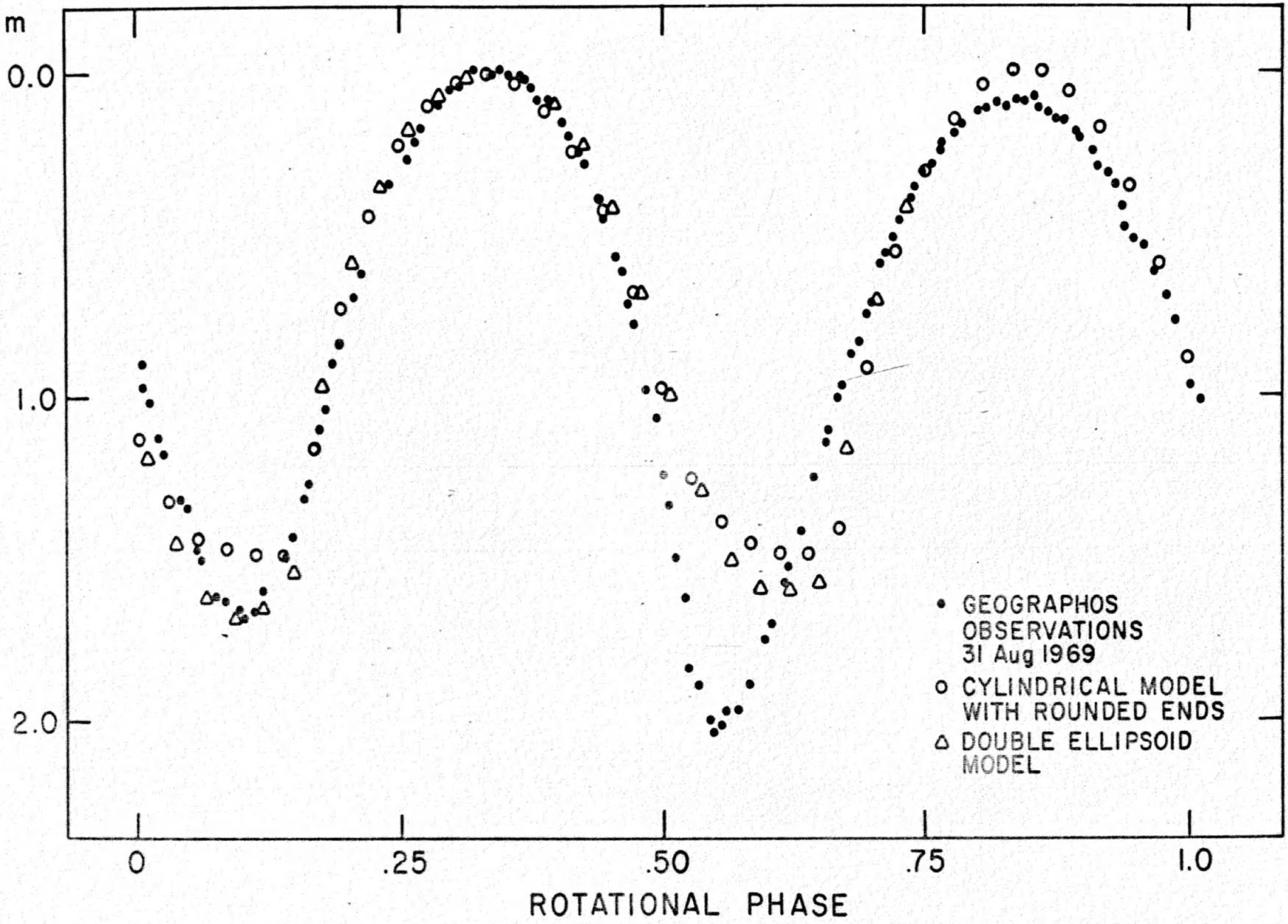

Fig. 10. Geographos and model 13 and 14 comparison; pole at (200°, 60°) ecliptic longitude and latitude respectively.

serious error, since it is defined for a spherical body which Geographos clearly is not.

Table III, column 5 or 6 reveals that the maxima of the model lightcurves exhibit a time-shift. These were obtained by subtracting the time (in degrees) of each model lightcurve maximum from the time of the maximum of the lightcurve at 90° aspect, 90° obliquity, and 20° phase, for which the expected absolute time-shift from the time of seeing a true maximum projected cross-sectional area at the detector was nearly zero. (For model 7 observations of obliquities from -90° to -180°, the subtractions were from 90° aspect, -90° obliquity and 20° phase.) As a further comparison between the models and Geographos, these model 7 time-shifts were used in place of the customary phase shift to determine the sidereal period and pole of Geographos. The method combines the techniques of the earlier amplitude comparison with the "routine" method, only now the time-shift (T) is expressed as a function of aspect, obliquity and phase. A trial value for the pole is assumed and laboratory coordinates are computed as before for each observation.

The sign of the time-shift is determined from the astrocentric longitude of the sub-earth point (L_e) and sub-solar point (L_s) as follows:

If $L_s - L_e \neq 0^\circ$, then

T is + when $0^\circ < (L_s - L_e) < 180^\circ$

or $-360^\circ < (L_s - L_e) < -180^\circ$

and T is - when $180^\circ < (L_s - L_e) < 360^\circ$

or $-180^\circ < (L_s - L_e) < 0^\circ$

If $L_s - L_e = 0^\circ$, then $T = 0^\circ$.

If $L_s - L_e = \pm 180^\circ$, the pole must lie on the great circle

joining the sub-earth and sub-solar points and lie between these points. In this case the sign of T is indeterminate, but if a lightcurve was actually made under these conditions, it would either be inverted (see Sec. III) or would have such a small amplitude that no accurate epoch could be obtained.

To avoid the lengthy interpolation used for the amplitude comparison, an attempt was made to find a function for T in terms of phase, aspect and obliquity. It was noted that the angle 1/2 δ (see Fig. 9) had the right properties for T, and in fact, $T = 1/2\ \delta \pm 2^{\circ}$ for all the model 7 data. Consequently, T was computed as 1/2 δ, where

$$\tan \delta/2 = \left[\frac{\sin (S - \beta) \sin (S - E)}{\sin (S - \alpha) \sin (S)}\right]^{1/2} \qquad (9)$$

where $S = 1/2\ (\alpha + \beta + E)$

and α = phase angle

$\beta = 90^{\circ} - \Theta$

$E = 90^{\circ} - \phi$

and Θ and ϕ are the same angles as defined earlier. The time-shift so obtained was added to the astrocentric longitude of the sub-earth point (L_e) for each observation and for each trial position of the pole. The remainder of the analysis was completed as usual. Table VII lists the average residuals for the sidereal period in the region of ecliptic longitude and latitude near the minimum, which occured at (200°, 60°).

For this pole, the lightcurve shapes, amplitudes and the sidereal period are in good agreement. It would not have been possible to obtain this solution without the model data. The shape of Geographos, therefore, is elongated. It is about three times

TABLE VII. AVERAGE RESIDUALS
IN THE SIDEREAL PERIOD FOR GEOGRAPHOS

Long. / Lat.	180°	200°	220°
50°	77 [a]	55	47
60°	39	37	49
70°	64	45	38

[a] Only the last two digits are listed; 77 is $^{d}.00000077$.

longer than it is wide, but it does not appear possible to distinguish any further characteristics without more observations to get better precision in the pole.

VII. CONCLUSION

This study has dealt exclusively with the problem of determining the shape of asteroids whose lightcurves suggest that the effects of differences in reflectivity over the surface are small or of secondary importance in determining the light variation. Comparison of the model data with the lightcurves of Hektor and Geographos has shown that simple shapes are consistent with the observations; however, this does not necessarily rule out more complicated ones. Notice, for example, that there is a 20° difference between the pole of Hektor as determined from the model data and as found from fitting a sidereal period to the time intervals between epochs. Is this difference due to an incorrect model or are there time-shifts in the epochs that have not been accounted for? How does one explain the roughness (variations $\simeq 0^{m}.03$ near maxima) of the Hektor lightcurves? Can both of these effects be explained by a more complicated shape than has been tried? Or is the shape simple and the surface complex? While this preliminary investigation does not attempt to answer these questions, the following is a list of important conclusions from the present study.

1. Amplitude-aspect relations may be used to give an approximate pole ($\pm 10^{\circ}$) provided the maximum amplitude (observed or extrapolated) is $\geq 0^{m}.4$ and the phase angles are $\leq 20^{\circ}$. (See Fig. 7).

2. The pole must be determined precisely before conclusions can be drawn about the shape, although an elongation primarily along

one axis may be detected from the degree of constancy of the absolute magnitude of the lightcurve maxima.

3. If an object is observed over a wide range of phase and aspect, then an approximate pole may be determined with model data using amplitude as a function of aspect, obliquity and phase (Sec. V B). Since the function also depends on the shape of the model, a further test of the model's ability to reproduce the overall shape of the observed lightcurves is necessary.

4. The time-shifts of the maxima of the model lightcurves are quite similar (equation 9) and may be used to obtain the orientation of the rotation axis and the sidereal period (Sec. V B), with two qualifications:

a. The model time-shifts have exceptionally large scatter when the rotation axis is near the sub-solar point. This is partly due to the small amplitude and the corresponding difficulty in identifying epochs, and also to the peculiar nature of the reflecting surface.

b. The time-shifts of models 1 and 9 (double bodies) deviated significantly from the average at 35° aspect regardless of the obliquity, which must be due to the effect of such a model shadowing itself.

The reason that most of the model time-shifts are represented by $\delta/2$ (see Fig. 9) may be qualitatively understood as a result of their approximately cylindrical shapes and a nongeometric scattering surface. Consider a meridian section of a model in the plane of the rotation axis and perpendicular to its long axis. This section has a nearly circular shape for most of the models. A "true" maximum

will occur whenever the sub-earth point lies on this meridian, at any latitude. Then the projected area is greatest as seen from the earth. If the scattering is geometric, this would be when the maximum was actually observed; however, the observed maximum is shifted $\delta/2$ from this condition. In the limiting situations for 90° aspect, the sub-earth and sub-solar points lie in the meridian section for 90° obliquity, or are inclined at 90° to it for 0° obliquity. In the former case, $\delta/2 = 0$ and there is no time-shift. In the latter case, $\delta/2 = \alpha/2$; the time-shift is just half of the phase angle. This means that at the time that the maximum is observed, a radius of the circular meridian section bisects the phase angle, and the surface element having this normal is reflecting light with the angle of emergence equal to the angle of incidence, and both angles lie in the same plane. Furthermore, because of the cylindrical nature of the models, there are many other normals and corresponding surface elements in this same condition (or nearly the same, since the light source and detector were at a finite distance from the model). A similar condition occurs at $\delta/2$ for intermediate aspects and obliquities, but in general, the angle of emergence is not equal to the angle of incidence, especially at larger phase angles.

More work should be done with models to investigate more closely the relationship between the shape, the surface texture, and the resulting time-shift. Is there a dependence of the time-shift on elongation, especially when the elongation is small? And what changes are made when reflectivity differences are included?

For future analysis of shape dominated lightcurves (see Table I, Class I and possibly also Class II), the present results suggest that equation (9) may be used as a first approximation for the

time-shifts of epochs of maximum light, except when a near-polar aspect is suspected (lightcurve amplitude is very small, or the shape of the lightcurve is peculiar). Once a rotation axis has been obtained (avoiding epochs with near-polar aspects), laboratory coordinates can be determined for each observation, and a simple model can be constructed and observed at these laboratory coordinates to see if the overall lightcurve shape and amplitude are reproduced. If so, the model can be further changed, if necessary, to attempt to reproduce the additional details in the lightcurves. (Table IV may be helpful to decide what changes to make.) Because this kind of trial and error analysis is so time consuming, one should investigate the possibility of using a computer to generate the model lightcurves. Different shapes and scattering laws would be relatively easy to model; however, the surface texture might have to be done with real surfaces.

ACKNOWLEDGMENTS

This work was supported by a grant from the National Geographic Society. I am indebted to several colleagues at the Lunar and Planetary Laboratory for their help in obtaining the model data, and especially to M. Howes for doing most of the programming, and to C. KenKnight for valuable assistance with the reductions. I also wish to thank my patient and perseverant wife for typing this manuscript.

REFERENCES

Coyne, G.V. and Gehrels, T. 1967, Astron. J. 72, 888.

Cook, A.F. 1971, in Physical Studies of Minor Planets, ed. T. Gehrels, (NASA SP - 267), p.155.

Dunlap, J.L. and Gehrels, T. 1969, Astron. J. 74, 796.

Dunlap, J.L. 1971, in Physical Studies, p.133.

Dunlap, J.L. 1972, Astron. J. (in preparation).

Russell, H.N. 1906, Astrophys. J. 24, 1.

Taylor, R.C. 1971, Physical Studies, p.147.

Van Houten, C.J. 1965, Hemel Dampkring 63, 162; Sterne Weltraum (1963) 2, 228.

Vesely, C.D. 1971, Physical Studies, p.133.

Widorn, Th. 1952, Mitt. Univ. - Sternw. Wien, 5, 19.

Zellner, B. 1972, Astrophys. J. Letters, 174, June 1, L 107.